


# ***d*-Mon: A Transmon with Strong Anharmonicity Based on Planar *c*-Axis Tunneling Junction between *d*-Wave and *s*-Wave Superconductors**

Hrishikesh Patel<sup>✉</sup>, Vedangi Pathak<sup>✉</sup>, Oguzhan Can, Andrew C. Potter, and Marcel Franz  
 Department of Physics and Astronomy, and Quantum Matter Institute, University of British Columbia,  
 Vancouver, British Columbia, Canada V6T 1Z1

 (Received 8 August 2023; revised 23 November 2023; accepted 7 December 2023; published 5 January 2024)

We propose a novel qubit architecture based on a planar *c*-axis Josephson junction between a thin flake *d*-wave superconductor, such as a high- $T_c$  cuprate  $\text{Bi}_2\text{Sr}_2\text{CaCu}_2\text{O}_{8+x}$ , and a conventional *s*-wave superconductor. When operated in the transmon regime the device—that we call “*d* mon”—becomes insensitive to offset charge fluctuations and, importantly, exhibits at the same time energy level spectrum with strong anharmonicity that is widely tunable through the device geometry and applied magnetic flux. Crucially, unlike previous qubit designs based on *d*-wave superconductors the proposed device operates in a regime where quasiparticles are fully gapped and can be therefore expected to achieve long coherence times.

DOI: [10.1103/PhysRevLett.132.017002](https://doi.org/10.1103/PhysRevLett.132.017002)

**Introduction.**—The transmon qubit, based on a superconducting Josephson junction shunted by a large capacitance [1], is the workhorse component powering the majority of intermediate scale quantum computers currently in operation. This includes the Google 54-qubit Sycamore processor [2], IBM 127-qubit Eagle processor [3], and 80-qubit Aspen-M-2 processor by Rigetti [4]. Transmon’s chief advantage over other superconducting qubit architectures is the insensitivity of its active energy levels to the fluctuations in the offset charge  $n_g$  that are typically difficult or impossible to control. This insensitivity, however, comes at a price: the energy spectrum of the transmon is only weakly anharmonic which imposes limits on the speed of operation due to the possibility of escape from the code space formed by the two lowest energy eigenstates [5–7].

We propose here a transmon variant that retains the offset charge insensitivity of the original device but has an arbitrarily large and easily tunable energy level anharmonicity. The key to this advance is the usage of a Josephson junction between superconductors with orthogonal order parameter symmetries. In this Letter we specifically consider junctions comprised of a *d*-wave and an *s*-wave superconductor, but the idea is applicable more generally. As is well known ordinary Cooper pair tunneling is symmetry prohibited across a *c*-axis *d*/*s* Josephson junction [8]. The leading process that enables passage of supercurrent is cotunneling of two Cooper pairs that results in the anomalous  $\pi$ -periodic current-phase relation (CPR),  $I(\varphi) \simeq I_{c2} \sin(2\varphi)$ . We will demonstrate below that the underlying  $\pi$ -periodic Josephson free energy  $F(\varphi)$  and its two degenerate minima at  $\varphi = \pm\pi/2$  enable the above mentioned key features of *d*-mon qubit.

The basic *d*-mon design is illustrated in Fig. 1(a) and consists of a very thin (several monolayers) *d*-wave flake resting on a large *s*-wave superconducting substrate.

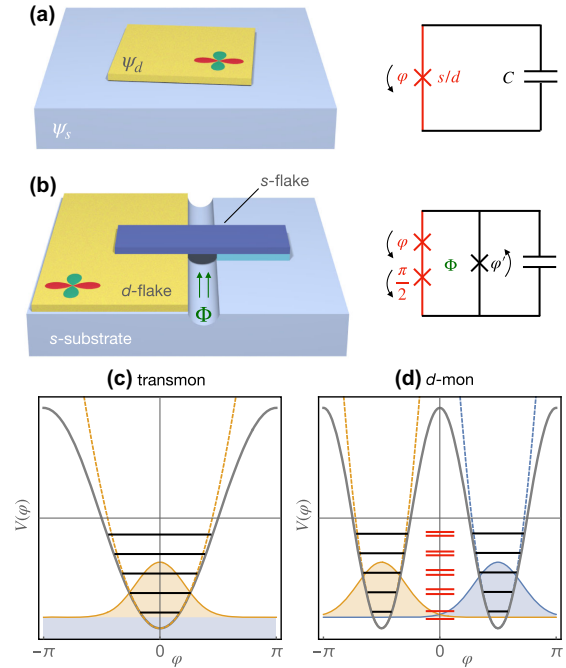


FIG. 1. Schematic of the proposed *d*-mon device. (a) Basic *d*-mon architecture and its circuit representation with one *s*/*d* junction and a capacitor  $C$ . (b) Split *d* mon: A large *d*SC flake resting on top of an *s*-wave substrate. A small *s*-wave flake bridges the gap threaded by magnetic flux  $\Phi$ . (c) Energy levels for an ordinary transmon are close to those of a harmonic well. (d) In *d* mon two sets of such levels belonging to separate wells of the  $\cos(2\varphi)$  potential weakly hybridize and produce a highly anharmonic spectrum represented by red lines.

High- $T_c$  cuprate  $\text{Bi}_2\text{Sr}_2\text{CaCu}_2\text{O}_{8+x}$  (BSCCO) is a well established  $d$ -wave superconductor ( $d$ SC) which has been recently exfoliated down to a monolayer thickness (while retaining its high critical temperature  $\sim 90$  K) [9] and would be a natural material for the flake. As a matter of principle the  $s$ -wave substrate can be fabricated of any conventional superconductor. However, as we discuss in more detail below, a material compatible with BSCCO—in that it can proximity induce a significant nodal gap—is required for practical qubit operation.

The Ginzburg-Landau (GL) free energy of the system depicted in Fig. 1(a) can be written as

$$F[\psi_s, \psi_d] = F_s[\psi_s] + F_d[\psi_d] + A|\psi_s|^2|\psi_d|^2 + B(\psi_s\psi_d^* + \text{c.c.}) + D(\psi_s^2\psi_d^{*2} + \text{c.c.}), \quad (1)$$

where  $\psi_{s/d}$  are complex scalar order parameters and  $F_{s/d}$  denote GL free energies of the individual superconductors. If both superconductors obey tetragonal symmetry then, importantly, the coefficient  $B$  is required to vanish. This is because under  $C_4$  rotation  $\psi_s \rightarrow \psi_s$  while  $\psi_d \rightarrow -\psi_d$ . In this situation the leading Josephson coupling arises from the last term in Eq. (1), which is allowed by symmetry and represents coherent tunneling of two Cooper pairs across the junction. Denoting the phase difference between two order parameters by  $\varphi$  the resulting Josephson free energy becomes

$$F(\varphi) = F_0 + 2D|\psi_s|^2|\psi_d|^2 \cos 2\varphi, \quad (2)$$

where  $F_0$  contains terms independent of  $\varphi$ . We note that although symmetry alone does not fix the sign of  $D$  many microscopic models, including the standard weak-coupling BCS theory, give  $D > 0$  which leads to the free energy landscape with two minima at  $\varphi = \pm\pi/2$ . Figures 1(c) and 1(d) illustrate the origin of the highly anharmonic spectrum in a junction with such  $\pi$ -periodic potential.

In reality BSCCO and other high- $T_c$  cuprates, such as  $\text{YBa}_2\text{Cu}_3\text{O}_{7-x}$  (YBCO), are weakly orthorhombic (that is,  $C_4$  is weakly broken down to  $C_2$  [10]). In this case coefficient  $B$  in the free energy (1) will be nonzero, but we expect it to be small such that the Josephson free energy is still dominated by the  $\cos 2\varphi$  term. The  $B$  term gives conventional  $2\pi$  periodic contribution to  $F(\varphi)$  proportional to  $\cos \varphi$ . At the level of the Josephson free energy the physics of  $d$  mon is therefore similar to the twisted bilayer of  $d$ -wave flakes which has been predicted to form a  $\mathcal{T}$ -broken  $d \pm id'$  phase at twist angles close to  $45^\circ$  [11]. Experimental evidence for such a state has been recently reported in twisted BSCCO bilayers [12]. Some important differences between the two setups include the fact the relative strength of the  $\cos \varphi$  in twisted  $d$ -wave bilayers can be controlled by the twist angle  $\theta$ . Also, the  $d \pm id'$  phase is topological (characterized by Chern number  $\pm 2$ ), and has gapless topological edge modes that may act as a source of

decoherence for a qubit device. By contrast, the  $d \pm is$  phase that is adiabatically connected to a pure  $s$ -wave superconductor, is topologically trivial.

*Anharmonicity from double-well free energy.*—Taking into account the junction charging energy the Hamiltonian for the  $d$  mon can be written as

$$H_\varphi = 4E_C(\hat{n} - n_g)^2 + E_J \cos 2\varphi + \delta U(\varphi), \quad (3)$$

where  $E_C = e^2/2C$  is the charging energy of the junction with capacitance  $C$ ,  $\hat{n} = -i\partial_\varphi$  is the Cooper pair number operator,  $E_J$  denotes the junction Josephson energy, and  $n_g$  is the offset charge. The potential  $\delta U$  is given by

$$\delta U(\varphi) = -\eta E_J (\cos \phi_{\text{ex}} \cos \varphi - \sin \phi_{\text{ex}} \sin \varphi). \quad (4)$$

The first term in  $\delta U$  represents the residual single-pair tunneling caused, e.g., by weakly broken  $C_4$  symmetry discussed above. The second term breaks  $\mathcal{T}$  explicitly—it makes the double-well asymmetric—and could arise from external magnetic flux  $\Phi$  in the split  $d$ -mon design depicted in Fig. 1(b) and discussed in more detail below. We are interested in the transmon regime characterized by  $E_J \gg E_C$  and a situation when  $\delta U$  represents a small perturbation, that is,  $|\eta| \lesssim 1$ .

Consider first the case  $\eta = 0$ . In this limit it is easy to see that the Hamiltonian (3) conserves the Cooper parity  $\mathcal{P} = (-1)^{\hat{n}}$ . In each parity sector the eigenstates and energy eigenvalues can be obtained analytically in terms of Mathieu functions as originally discussed in Ref. [1]. In the transmon regime  $E_J \gg E_C$  an accurate approximation for the splitting between the two lowest energy levels can be derived [13],

$$\Delta E \simeq 16E_C \sqrt{\frac{2}{\pi}} \left( \frac{2E_J}{E_C} \right)^{3/4} e^{-\sqrt{2E_J/E_C}} \cos(\pi n_g). \quad (5)$$

Band crossings at half-integer values of  $n_g$  in Eq. (5) are exact and follow from parity conservation.

We will be interested primarily in the case of nonzero  $\eta$  when  $\mathcal{P}$  conservation no longer applies. In this case analytical results are not available, but it is possible to solve the problem numerically by representing the Hamiltonian (3) as a matrix in the Cooper pair number basis  $|n\rangle = e^{in\varphi}/\sqrt{2\pi}$  with  $n$  integer. We truncate the infinite Hamiltonian matrix  $H_{nm} = \langle n|H|m\rangle$  according to  $|n|, |m| \leq n_{\text{max}}$  and diagonalize the resulting matrix of size  $2n_{\text{max}} + 1$ . We find that calculations become fully converged for  $n_{\text{max}} \geq 15$ . As shown in Fig. 2(a) for  $\eta = 0$  the energy levels behave in accord with the analytical result [Eq. (5)]. Note that the relevant wave functions  $\psi_j(\varphi)$  with  $j = 0, 1$  can be classified as symmetric and antisymmetric with respect to the  $\varphi = 0$  origin only for integral  $n_g$ . More

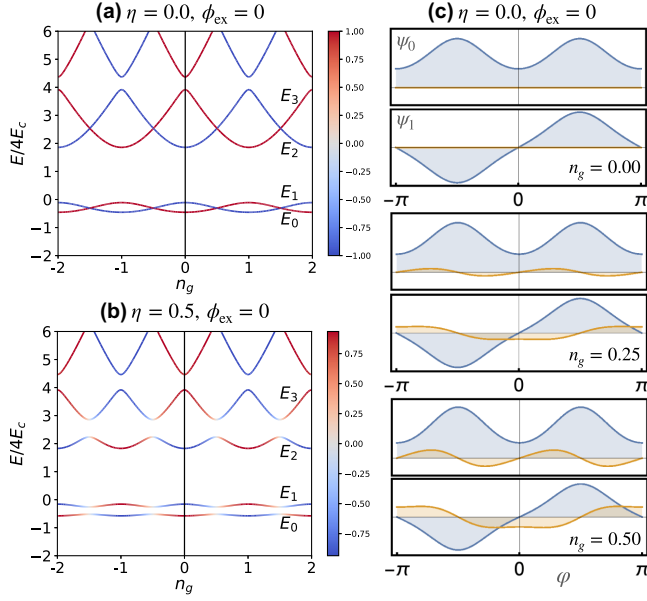


FIG. 2. Energy levels and wave functions of the  $d$ -mon Hamiltonian (3) for  $E_J/E_C = 8$ . (a),(b) Lowest energy levels as a function of offset charge  $n_g$ . The color represents parity  $\langle \mathcal{P} \rangle \in (-1, 1)$ . (c) Wave functions  $\psi_0(\phi)$  and  $\psi_1(\phi)$  belonging to the two lowest energies for selected values of  $n_g$ . Blue (orange) lines represent real (imaginary) parts of  $\psi_j$ .

generally they also contain an imaginary part that has opposite symmetry [Fig. 2(c)].

When  $\eta \neq 0$  the parity-protected energy crossings are lifted [Fig. 2(b)]. As a result, the low-lying energy bands flatten out—the qubit becomes insensitive to the offset charge fluctuations in the same way as the original transmon. Importantly, in

$d$  mon this feature does *not* come at the expense of anharmonicity. This is illustrated in Fig. 3: Although the detailed behavior depends on the relative amplitude of the two terms comprising  $\delta U$ , in nearly all cases, one can achieve large anharmonicity, while the energy levels remain essentially independent of  $n_g$ , as measured by the flatness indicator  $f$  defined as  $f = w_1/\omega_{10}$ , where  $w_j$  denotes the bandwidth of the  $j$ th band and  $\omega_{ij} = E_i - E_j$ . The anharmonicity is measured by parameter  $\alpha_r = (\omega_{21} - \omega_{10})/\omega_{20}$ . An inspection of Fig. 3(d) reveals that for  $E_J/E_C \gtrsim 20$  bands become extremely flat, and by adjusting the flux  $\phi_{\text{ex}}$  one can always achieve significant level anharmonicity. The limit of zero flux is special: Here the bands become flat but remain nearly degenerate. This is because, as discussed in the Supplemental Material [14],  $\langle \psi_1 | \cos \phi | \psi_0 \rangle = 0$ , and hence  $\delta U$  has no effect to leading order in perturbation theory. On the other hand  $\langle \psi_1 | \sin \phi | \psi_0 \rangle \neq 0$  which implies that  $\delta U$  is much more effective at splitting the bands at nonzero  $\phi_{\text{ex}}$ . Additional results characterizing convergence and various parameter regimes of the Hamiltonian (3) are given in the Supplemental Material [14].

**Quasiparticles.**—Because of their reliance on  $ab$ -plane junctions a significant drawback of some earlier cuprate-based qubit designs [19–22] was the presence of quasiparticles that survive in the vicinity of the Dirac nodes in their  $d$ -wave order parameter down to arbitrarily low energies [23,24]. As we now explain the thin  $d$ SC flake in Fig. 1(a) becomes a  $d \pm is$  superconductor whose quasiparticles are gapped everywhere on its Fermi surface.

The microscopic Hamiltonian for electrons near the  $d/s$  interface can be written as  $\mathcal{H}_{\text{el}} = \sum_k \Psi_k^\dagger H_k \Psi_k$  with

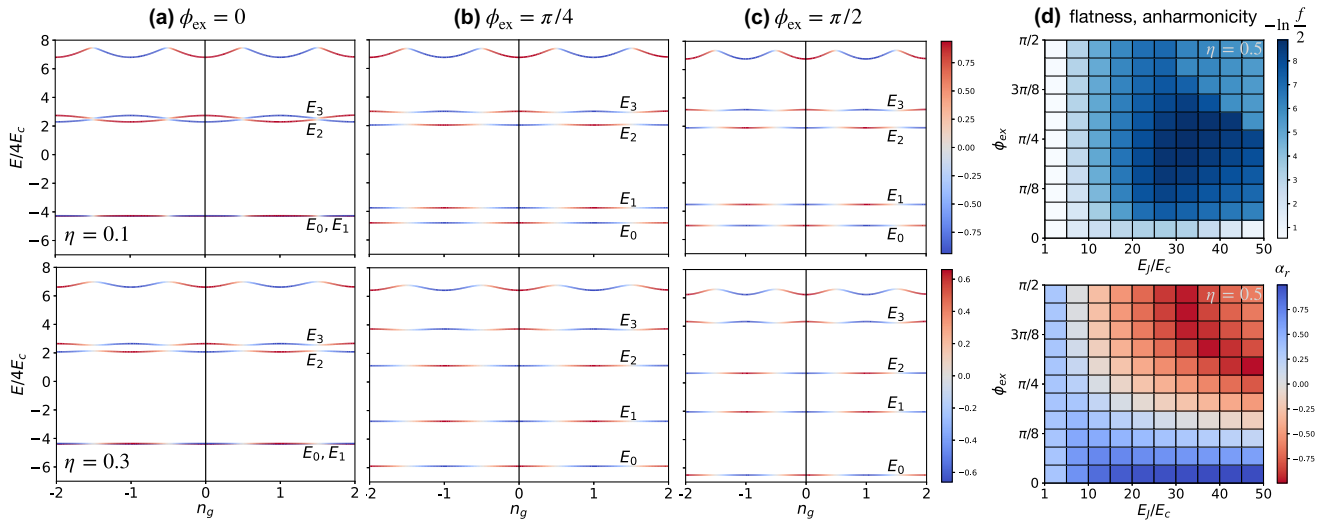


FIG. 3. Characteristic  $d$ -mon properties. (a)–(c) Lowest energy eigenvalues as a function of the offset charge  $n_g$  for  $E_J/E_C = 32$  and representative values of parameters  $\eta$  and  $\phi_{\text{ex}}$ . (d) Band flatness  $f$  and relative level anharmonicity  $\alpha_r$ , both defined in the text. Large values of  $-\ln(f/2)$  indicate very flat bands whereas values of  $\alpha_r$  away from 0 signal anharmonicity, which can be both positive or negative. All results shown are for  $n_{\text{max}} = 15$  which corresponds to fully converged numerics.

$\Psi_k = (c_{k\uparrow}, c_{-k\downarrow}^\dagger; s_{k\uparrow}, s_{-k\downarrow}^\dagger)^T$  and

$$H_k = \begin{pmatrix} \xi_k & \Delta_k & t_k & 0 \\ \Delta_k & -\xi_k & 0 & -t_k \\ t_k & 0 & \xi_k^s & e^{i\varphi} \Delta_s \\ 0 & -t_k & e^{-i\varphi} \Delta_s & -\xi_k^s \end{pmatrix}. \quad (6)$$

Here  $c_{k\sigma}^\dagger, s_{k\sigma}^\dagger$  denote electron creation operators in  $d$  and  $s$  layers, respectively,  $\xi_k, \xi_k^s$  are the corresponding normal-state dispersions referenced to the Fermi level  $\mu$ , and  $\Delta_k = \Delta_d \cos(2\alpha_k)$  is the  $d$ -wave gap function with  $\alpha_k$  the polar angle of the momentum vector  $k$ ;  $\Delta_s$  denotes the  $k$ -independent  $s$ -wave gap.

We now imagine integrating out the gapped fermion degrees of freedom in the  $s$ -wave layer, assuming weak interlayer coupling  $t_k$  (see the Supplemental Material [14] for the details of the procedure). The resulting effective Hamiltonian for the remaining  $c$  fermions takes the form

$$\mathcal{H}_{\text{eff}} = \sum_k \psi_k^\dagger \begin{pmatrix} \tilde{\xi}_k & \Delta_k + e^{i\varphi} m_s \\ \Delta_k + e^{-i\varphi} m_s & -\tilde{\xi}_k \end{pmatrix} \psi_k, \quad (7)$$

with  $\psi_k = (c_{k\uparrow}, c_{-k\downarrow}^\dagger)^T$ . The tilde on  $\xi_k$  means that the bare dispersion has been modified while  $m_s \approx t^2/\Delta_s$  denotes the proximity induced gap. For a fixed classical phase  $\varphi$  the quasiparticle spectrum of  $\mathcal{H}_{\text{eff}}$  reads as

$$E_k = \pm \sqrt{\tilde{\xi}_k^2 + |\Delta_k + e^{i\varphi} m_s|^2}. \quad (8)$$

Classically, in the absence of fluctuations, the system will reside in one of the minima of the free energy (2) with  $\varphi = \pm\pi/2$ . This results in the  $d \pm is$  superconductor with a minimum gap  $m_s$  to all quasiparticle excitations.

We see that at the mean-field level (that is, neglecting fluctuations in the phase  $\varphi$ )  $d$  mon is protected from quasiparticle poisoning by the proximity gap  $m_s$ . Of course in order for the device to function as a useful qubit we must allow for  $\varphi$  to undergo quantum fluctuations. Mathematically, we need to reintroduce the charging energy  $E_C$  and permit the phase variable to tunnel between the two potential minima.

An important question thus arises: Will the quasiparticle gap survive in the presence of such quantum fluctuations? We tackle this question in the Supplemental Material [14]. Employing two different methods (a perturbative treatment and a more elaborate semiclassical dilute instanton approximation) we conclude that the quasiparticle gap survives even though it is reduced to

$$\tilde{m}_s = m_s |\langle \psi_0 | \sin \varphi | \psi_1 \rangle| \simeq m_s e^{-\sqrt{E_C/4E_J}}, \quad (9)$$

where  $\psi_j(\varphi)$  are eigenstates of the phase Hamiltonian (3). An evaluation of the matrix element shows that phase

fluctuations lead to a relatively modest gap suppression (between 5% and 20%) in the transmon regime. Intuitively, this can be understood by considering the structure of wave functions  $\psi_j(\varphi)$  depicted in Fig. 2: Thinking semiclassically the phase particle spends most of its time in the vicinity of the classical minima at  $\pm\pi/2$  where the quasiparticle gap is maximal and only makes short excursions to the neighborhood of  $\varphi = 0, \pi$  where the quasiparticles are gapless. The  $e^{-\sqrt{E_C/4E_J}}$  factor reflects small quantum fluctuations about these minima. Larger values of  $E_J/E_C$  (likely relevant for practical implementations of the  $d$  mon) suppress these fluctuations and concentrate the phase wave functions near the minima, leaving a negligible amplitude near  $\varphi = 0, \pi$ .

*Split  $d$ -mon.*—In the basic  $d$ -mon realization depicted in Fig. 1(a) it is possible to control some system parameters by adjusting the flake size. This follows from the fact that  $E_J \sim \mathcal{A}$ , the interface area,  $\mathcal{A}$ , while  $E_C \sim \mathcal{A}^{-1}$ . On the other hand, in the absence of explicit  $\mathcal{T}$  breaking  $\phi_{\text{ex}}$  is fixed to zero, and the  $\eta$  parameter is set by the material properties of the junction and cannot be easily controlled. Hence this basic design can access only a small portion of the parameter space afforded by the Hamiltonian (3).

To gain more flexibility we take inspiration from the split transmon architecture [1] and Ref. [20] and consider a three-junction device depicted in Fig. 1(b). We assume that the large  $s/d$  junction has negligible charging energy, and its phase is therefore permanently locked to one of the  $\mathcal{T}$  breaking minima (hereafter we assume  $+\pi/2$  for concreteness). The charging energy of the small  $s$ -wave flake is non-negligible, and phases  $\varphi$  and  $\varphi'$  are allowed to fluctuate. In the small inductance limit the loop cannot trap any self-induced flux, and the two phases are constrained by the single-valuedness of the wave function such that  $\varphi + \varphi' + \pi/2 = 2\pi\Phi/\Phi_0$ , where  $\Phi_0 = hc/2e$  denotes the flux quantum. If we define  $\phi_{\text{ex}} = 2\pi\Phi/\Phi_0 - \pi/2$  then the total Josephson energy can be written as  $U(\varphi) = E_J \cos 2\varphi - E_S \cos(\phi_{\text{ex}} - \varphi)$  where  $E_S$  denotes the Josephson energy of the  $s/s$  junction. By expanding the second cosine one finds that  $U(\varphi)$  coincides with the potential in the Hamiltonian (3) if one identifies  $\eta = E_S/E_J$ . We conclude that the split  $d$ -mon architecture Fig. 1(b) is capable of realizing the entire range of properties represented by the Hamiltonian [Eq. (3)].

*Conclusions.*—A Josephson junction formed at the interface between  $d$ - and  $s$ -wave superconductors displays anomalous  $\pi$ -periodic CPR which underlies its proposed functionality as an improved transmon qubit. We demonstrated that the resulting “ $d$  mon” is robust to offset charge fluctuations while at the same time exhibits a large and easily tunable level anharmonicity. Similar to the original transmon [1], control and readout can be efficiently performed using microwave pulses. Importantly, unlike many previous proposals based on  $d$ SCs, we showed that the  $d$  mon operates in the regime of fully gapped



quasiparticles which is essential to prevent decoherence effects. Several conditions on system parameters must be met for the device to function as a practical qubit. At a minimum, one requires a high-transparency  $d/s$  interface that would facilitate a significant Cooper pair cotunneling amplitude and proximity generate a sizeable nodal gap  $m_s$  to protect against quasiparticle poisoning. At temperature scales much lower than  $m_s$ , thermal fluctuations and fluctuations in the amplitude of the order parameter will also be negligible.

Even though  $c$ -axis junctions formed of various high- $T_c$  cuprates have been extensively studied [25]—culminating in recent works on twisted BSCCO junctions [12,26–29]—not much recent effort went into experimental studies of  $c$ -axis  $d/s$  junctions. Early experiments on  $c$ -axis junctions between cuprates (YBCO or BSCCO) and Pb [30–32] showed only conventional  $2\pi$  periodic CPR and were interpreted as evidence for  $s$ -wave superconductivity in cuprates. Given the obvious contradiction with the present-day consensus on  $d$ -wave symmetry [33], and the technological potential of  $\pi$ -periodic junctions discussed here, it is clearly important to revisit these results using modern techniques designed for ultraclean junction preparation [12,28,29]. An interesting possibility would be to explore interfaces between high- $T_c$  cuprates and iron-based superconductors such as  $\text{LaFeAsO}_{1-x}\text{F}_x$  or  $\text{SmFeAsO}_{1-x}\text{H}_x$ . The latter are layered tetragonal materials with an  $s$ -wave superconducting gap and critical temperatures of up to 50 K [34]. In addition they exhibit lattice constants ( $\sim 4$  Å) similar to cuprates thus potentially enabling fabrication of atomically clean  $c$ -axis junctions by means of mechanical exfoliation [9] or atomic layer-by-layer molecular beam epitaxy [35].

We note in closing that the  $\pi$ -periodic CPR that lies at the heart of our  $d$ -mon proposal can also be achieved in  $d$ SC bilayers with a near- $45^\circ$  twist angle [36] or, using more conventional ingredients [37,38], as recently implemented in voltage-controlled semiconductor nanowire Josephson junctions [39]. These platforms could also be harnessed to produce an improved transmon with large anharmonicity. The proposed  $s/d$  junction does not require precise twist-angle control and could thus be fabricated using molecular beam epitaxy. In the long term this may confer a technological advantage over twisted  $d$ SC bilayers which must be prepared very near the  $45^\circ$  twist angle to exhibit  $\pi$ -periodic CPR.

The authors are indebted to C.-K. Chiu, P. Kim, G. Refael, N. Poccia, and U. Vool for stimulating discussions and correspondence. The work was supported by NSERC, CIFAR and the Canada First Research Excellence Fund, Quantum Materials and Future Technologies Program. A. C. P. was supported by the US Department of Energy DOE DE-SC0022102, and in part by the Alfred

P. Sloan Foundation through a Sloan Research Fellowship. M. F. and A. C. P. thank Aspen Center for Physics where part of this work was completed.

- [1] Jens Koch, Terri M. Yu, Jay Gambetta, A. A. Houck, D. I. Schuster, J. Majer, Alexandre Blais, M. H. Devoret, S. M. Girvin, and R. J. Schoelkopf, Charge-insensitive qubit design derived from the Cooper pair box, *Phys. Rev. A* **76**, 042319 (2007).
- [2] Frank Arute, Kunal Arya, Ryan Babbush, Dave Bacon, Joseph C. Bardin, Rami Barends, Rupak Biswas, Sergio Boixo, Fernando G. S. L. Brandao, David A. Buell *et al.*, Quantum supremacy using a programmable superconducting processor, *Nature (London)* **574**, 505 (2019).
- [3] Youngseok Kim, Andrew Eddins, Sajant Anand, Ken Xuan Wei, Ewout van den Berg, Sami Rosenblatt, Hasan Nayfeh, Yantao Wu, Michael Zaletel, Kristan Temme, and Abhinav Kandala, Evidence for the utility of quantum computing before fault tolerance, *Nature (London)* **618**, 500 (2023).
- [4] Emanuele G. Dalla Torre and Matthew J. Reagor, Simulating the interplay of particle conservation and long-range coherence, *Phys. Rev. Lett.* **130**, 060403 (2023).
- [5] P. Krantz, M. Kjaergaard, F. Yan, T. P. Orlando, S. Gustavsson, and W. D. Oliver, A quantum engineer's guide to superconducting qubits, *Appl. Phys. Rev.* **6**, 021318 (2019).
- [6] Morten Kjaergaard, Mollie E. Schwartz, Jochen Braumüller, Philip Krantz, Joel I.-J. Wang, Simon Gustavsson, and William D. Oliver, Superconducting qubits: Current state of play, *Annu. Rev. Condens. Matter Phys.* **11**, 369 (2020).
- [7] Irfan Siddiqi, Engineering high-coherence superconducting qubits, *Nat. Rev. Mater.* **6**, 875 (2021).
- [8] R. A. Klemm, C. T. Rieck, and K. Scharnberg, Order-parameter symmetries in high-temperature superconductors, *Phys. Rev. B* **61**, 5913 (2000).
- [9] Yijun Yu, Liguang Ma, Peng Cai, Ruidan Zhong, Cun Ye, Jian Shen, G. D. Gu, Xian Hui Chen, and Yuanbo Zhang, High-temperature superconductivity in monolayer  $\text{Bi}_2\text{Sr}_2\text{CaCu}_2\text{O}_{8+\delta}$ , *Nature (London)* **575**, 156 (2019).
- [10] A. Bianconi, N. L. Saini, T. Rossetti, A. Lanzara, A. Perali, M. Messori, H. Oyanagi, H. Yamaguchi, Y. Nishihara, and D. H. Ha, Stripe structure in the  $\text{CuO}_2$  plane of perovskite superconductors, *Phys. Rev. B* **54**, 12018 (1996).
- [11] Oguzhan Can, Tarun Tummuru, Ryan P. Day, Ilya Elfimov, Andrea Damascelli, and Marcel Franz, High-temperature topological superconductivity in twisted double-layer copper oxides, *Nat. Phys.* **17**, 519 (2021).
- [12] S. Y. Frank Zhao, Nicola Poccia, Xiaomeng Cui, Pavel A. Volkov, Hyobin Yoo, Rebecca Engelke, Yuval Ronen, Ruidan Zhong, Genda Gu, Stephan Plugge, Tarun Tummuru, Marcel Franz, Jedediah H. Pixley, and Philip Kim, Emergent interfacial superconductivity between twisted cuprate superconductors, *Science* **382**, 1422 (2023).
- [13] W. C. Smith, A. Kou, X. Xiao, U. Vool, and M. H. Devoret, Superconducting circuit protected by two-cooper-pair tunneling, *npj Quantum Inf.* **6**, 8 (2020).
- [14] See Supplemental Material at <http://link.aps.org/supplemental/10.1103/PhysRevLett.132.017002> for additional numerical results, derivation of the effective qubit

- Hamiltonian, estimate of characteristic energy scales, and treatment of quasiparticle excitations, which includes Refs. [15–18].
- [15] Yugui Yao, Fei Ye, Xiao-Liang Qi, Shou-Cheng Zhang, and Zhong Fang, Spin-orbit gap of graphene: First-principles calculations, *Phys. Rev. B* **75**, 041401 (2007).
  - [16] Note that in a finite system, the minimum  $k$  is bounded below by  $\sim 1/L$ , so  $k = 0$  does not appear in the product, so that the product is nonvanishing for any finite  $L$  even though  $\lim_{k \rightarrow 0} \langle v_k^+ | v_k^- \rangle = 0$ .
  - [17] Alexander Altland and Ben D. Simons, *Condensed Matter Field Theory*, 2nd ed. (Cambridge University Press, Cambridge, England, 2010), [10.1017/CBO9780511789984](https://doi.org/10.1017/CBO9780511789984).
  - [18] J. Zinn-Justin, *Quantum Field Theory and Critical Phenomena*, International Series of Monographs on Physics (Oxford University Press, New York, 2021).
  - [19] Alexandre M. Zagorskin, A scalable, tunable qubit, based on a clean dnd or grain boundary d-d junction, [arXiv:cond-mat/9903170](https://arxiv.org/abs/cond-mat/9903170).
  - [20] Lev B. Ioffe, Vadim B. Geshkenbein, Mikhail V. Feigel'man, Alban L. Fauchère, and Gianni Blatter, Environmentally decoupled SDS-wave Josephson junctions for quantum computing, *Nature (London)* **398**, 679 (1999).
  - [21] Alexandre Blais and Alexandre M. Zagorskin, Operation of universal gates in a solid-state quantum computer based on clean Josephson junctions between d-wave superconductors, *Phys. Rev. A* **61**, 042308 (2000).
  - [22] M. H. S. Amin, A. Yu. Smirnov, A. M. Zagorskin, T. Lindström, S. A. Charlebois, T. Claeson, and A. Ya. Tzalenchuk, Silent phase qubit based on  $d$ -wave Josephson junctions, *Phys. Rev. B* **71**, 064516 (2005).
  - [23] Ya V Fominov, Alexandre Avraamovitch Golubov, and M Yu Kupriyanov, Decoherence due to nodal quasiparticles in  $d$ -wave qubits, *J. Exp. Theor. Phys. Lett.* **77**, 587 (2003).
  - [24] M. H. S. Amin and A. Yu. Smirnov, Quasiparticle decoherence in  $d$ -wave superconducting qubits, *Phys. Rev. Lett.* **92**, 017001 (2004).
  - [25] J. N. Eckstein and I. Bozovic, High-temperature superconducting multilayers and heterostructures grown by atomic layer-by-layer molecular beam epitaxy, *Annu. Rev. Mater. Sci.* **25**, 679 (1995).
  - [26] Jongyun Lee, Wonjun Lee, Gi-Yeop Kim, Yong-Bin Choi, Jinho Park, Seong Jang, Genda Gu, Si-Young Choi, Gil Young Cho, Gil-Ho Lee *et al.*, Twisted van der Waals Josephson junction based on a high- $T_c$  superconductor, *Nano Lett.* **21**, 10469 (2021).
  - [27] Yuying Zhu, Menghan Liao, Qinghua Zhang, Hong-Yi Xie, Fanqi Meng, Yaowu Liu, Zhonghua Bai, Shuaihua Ji, Jin Zhang, Kaili Jiang *et al.*, Presence of  $s$ -wave pairing in Josephson junctions made of twisted ultrathin  $\text{Bi}_2\text{Sr}_2\text{CaCu}_2\text{O}_{8+x}$  flakes, *Phys. Rev. X* **11**, 031011 (2021).
  - [28] Yejin Lee, Mickey Martini, Tommaso Confolone, Sanaz Shokri, Christian N. Saggau, Daniel Wolf, Genda Gu, Kenji Watanabe, Takashi Taniguchi, Domenico Montemurro, Valerii M. Vinokur, Kornelius Nielsch, and Nicola Poccia, Encapsulating high-temperature superconducting twisted van der Waals heterostructures blocks detrimental effects of disorder, *Adv. Mater.* **35**, 2209135 (2023).
  - [29] Mickey Martini, Yejin Lee, Tommaso Confolone, Sanaz Shokri, Christian N. Saggau, Daniel Wolf, Genda Gu, Kenji Watanabe, Takashi Taniguchi, Domenico Montemurro, Valerii M. Vinokur, Kornelius Nielsch, and Nicola Poccia, Twisted cuprate van der Waals heterostructures with controlled Josephson coupling, [arXiv:2303.16029](https://arxiv.org/abs/2303.16029).
  - [30] A. G. Sun, D. A. Gajewski, M. B. Maple, and R. C. Dynes, Observation of Josephson pair tunneling between a high- $t_c$  cuprate ( $\text{YBa}_2\text{Cu}_3\text{O}_{7-\delta}$ ) and a conventional superconductor (Pb), *Phys. Rev. Lett.* **72**, 2267 (1994).
  - [31] R. Kleiner, A. S. Katz, A. G. Sun, R. Summer, D. A. Gajewski, S. H. Han, S. I. Woods, E. Dantsker, B. Chen, K. Char, M. B. Maple, R. C. Dynes, and John Clarke, Pair tunneling from  $c$ -axis  $\text{YBa}_2\text{Cu}_3\text{O}_{7-x}$  to Pb: Evidence for  $s$ -wave component from microwave induced steps, *Phys. Rev. Lett.* **76**, 2161 (1996).
  - [32] M. Möhle and R. Kleiner,  $c$ -axis Josephson tunneling between  $\text{Bi}_2\text{Sr}_2\text{CaCu}_2\text{O}_{8+x}$  and Pb, *Phys. Rev. B* **59**, 4486 (1999).
  - [33] C. C. Tsuei and J. R. Kirtley, Pairing symmetry in cuprate superconductors, *Rev. Mod. Phys.* **72**, 969 (2000).
  - [34] Hideo Hosono, Akiyasu Yamamoto, Hidenori Hiramatsu, and Yanwei Ma, Recent advances in iron-based superconductors toward applications, *Mater. Today* **21**, 278 (2018).
  - [35] Anthony T. Bollinger, Xi He, Xiaotao Xu, Xiaoyan Shi, and Ivan Bozović, Method to create cuprate tunnel junctions with atomically sharp interfaces, *J. Vac. Sci. Technol. B* **40**, 015001 (2021).
  - [36] Valentina Brosco, Giuseppe Serpico, Valerii Vinokur, Nicola Poccia, and Uri Vool, following Letter, A superconducting qubit based on cuprate twisted Van der Waals heterostructures, *Phys. Rev. Lett.* **132**, 017003 (2024).
  - [37] B. Douçot and L. B. Ioffe, Physical implementation of protected qubits, *Rep. Prog. Phys.* **75**, 072001 (2012).
  - [38] Matthew T. Bell, Joshua Paramanandam, Lev B. Ioffe, and Michael E. Gershenson, Protected Josephson rhombus chains, *Phys. Rev. Lett.* **112**, 167001 (2014).
  - [39] T. W. Larsen, M. E. Gershenson, L. Casparis, A. Kringhøj, N. J. Pearson, R. P. G. McNeil, F. Kuemmeth, P. Krogstrup, K. D. Petersson, and C. M. Marcus, Parity-protected superconductor-semiconductor qubit, *Phys. Rev. Lett.* **125**, 056801 (2020).